# Control of Nonapoptotic Developmental Cell Death in *Caenorhabditis elegans* by a Polyglutamine-Repeat Protein

Elyse S. Blum, *et al.*

*Science* **335**, 970 (2012);
DOI: 10.1126/science.1215156



*Science* (print ISSN 0036-8075; online ISSN 1095-9203) is published weekly, except the last week in December, by the American Association for the Advancement of Science, 1200 New York Avenue NW, Washington, DC 20005. 

# Control of Nonapoptotic Developmental Cell Death in *Caenorhabditis elegans* by a Polyglutamine-Repeat Protein

Elyse S. Blum, Mary C. Abraham, Satoshi Yoshimura, Yun Lu, Shai Shaham*

Death is a vital developmental cell fate. In *Caenorhabditis elegans*, programmed death of the linker cell, which leads gonadal elongation, proceeds independently of caspases and apoptotic effectors. To identify genes promoting linker-cell death, we performed a genome-wide RNA interference screen. We show that linker-cell death requires the gene *pqn-41*, encoding an endogenous polyglutamine-repeat protein. *pqn-41* functions cell-autonomously and is expressed at the onset of linker-cell death. *pqn-41* expression is controlled by the mitogen-activated protein kinase kinase SEK-1, which functions in parallel to the zinc-finger protein LIN-29 to promote cellular demise. Linker-cell death is morphologically similar to cell death associated with normal vertebrate development and polyglutamine-induced neurodegeneration. Our results may therefore provide molecular inroads to understanding nonapoptotic cell death in metazoan development and disease.

Programmed cell death is essential for metazoan development and is required to sculpt organs, eliminate harmful cells, and counter cell division (*1*, *2*). Apoptosis, an extensively studied cell death process, requires caspase activation and is accompanied by a stereotypical morphological signature that includes chromatin compaction, cytoplasmic shrinkage, and no gross disruption of organelles (*3*). Mice lacking key apoptotic effectors such as caspase-3, caspase-9, Apaf-1, or Bax and Bak have mild defects and can survive to adulthood (*4*). Given the prevalence of cell death during mouse development (*5*), these observations raise the possibility that a nonapoptotic cell death pathway plays key roles in animal development. Although genes promoting necrotic cell death have been identified (*6*), they are not required for normal development (*7*). Indeed, genes dedicated to nonapoptotic developmental cell death have not been described.

We previously described the programmed death of the *Caenorhabditis elegans* linker cell during male reproductive system development (*8*). The linker cell leads the migration of the male gonad and dies between the fourth larval stage (L4) and adulthood (*9*). Linker cell demise is orchestrated by a cell-autonomous process independent of all *C. elegans* caspases and other known cell death genes (*8*, *10*). Electron microscopy (EM) of the dying linker cell reveals nonapoptotic features, including crenellation (indentation) of the nuclear envelope, uncondensed chromatin, and organelle swelling (Fig. 1C) (*8*). However, linker cell death does not require the unfolded protein response or other stress responses (tables S1 and S2). Similar morphological features are seen during normal developmental death of neurons in the vertebrate spinal cord and ciliary ganglion (*11*–*13*), suggesting that linker cell–type death is morphologically conserved.

Laboratory of Developmental Genetics, The Rockefeller University, 1230 York Avenue, New York, NY 10065 USA.

*To whom correspondence should be addressed. E-mail shaham@rockefeller.edu

To uncover the molecular mechanisms leading to linker cell death, we performed a genome-wide RNA interference (RNAi) screen to identify genes whose inactivation prevents linker cell death. We fed 18,132 bacterial clones, expressing double-stranded RNA (dsRNA) corresponding to 89% of predicted protein-coding *C. elegans* genes, individually to RNAi-sensitized males expressing a *lag-2* promoter::green fluorescent protein (GFP) linker cell reporter (*14*). The screen strategy was validated by recovery of the *lin-29* gene, previously identified as required for linker cell death (*8*). We recovered five additional RNAi clones leading to linker cell survival. Three clones also affect linker cell migration and may thus affect multiple aspects of linker cell fate. One of the remaining clones, derived from the gene *pqn-41* (Fig. 2A), caused linker cell survival in 20% of animals (Fig. 1A) with no obvious pleiotropic effects (fig. S1) and was further studied.

To confirm that the clone we identified inactivates *pqn-41*, we generated a deletion allele, *ns294*, in the gene. *pqn-41*(*ns294*) animals lack 337 nucleotides, removing portions of intron 17 and exon 18 of the predicted genomic structure (Fig. 2A). Consistent with our RNAi results, *pqn-41*(*ns294*) adult males possess an inappropriately surviving linker cell (Fig. 1, A and B). Furthermore, in *pqn-41*(*ns294*) mutants the linker cell persists at least 24 hours after the L4-adult transition (19% survival, $n$ = 79 animals), suggesting that reducing *pqn-41* function not only delays but may block linker cell death. RNAi against *pqn-41* in *pqn-41*(*ns294*) animals does not increase linker cell survival (16% survival, $n$ = 108 animals), suggesting that *ns294* may be a strong loss-of-function allele. To test whether *pqn-41*(*ns294*) mutants have defects in developmental apoptosis, we scored for surviving pharyngeal cells that normally die apoptotically (*15*) and observed none ($n$ = 10 animals). Thus, the nonapoptotic nature of linker cell death may reflect distinct molecular machineries.

None of the *pqn-41*(*ns294*) surviving cells exhibit nuclear crenellation ($n$ = 19 animals),

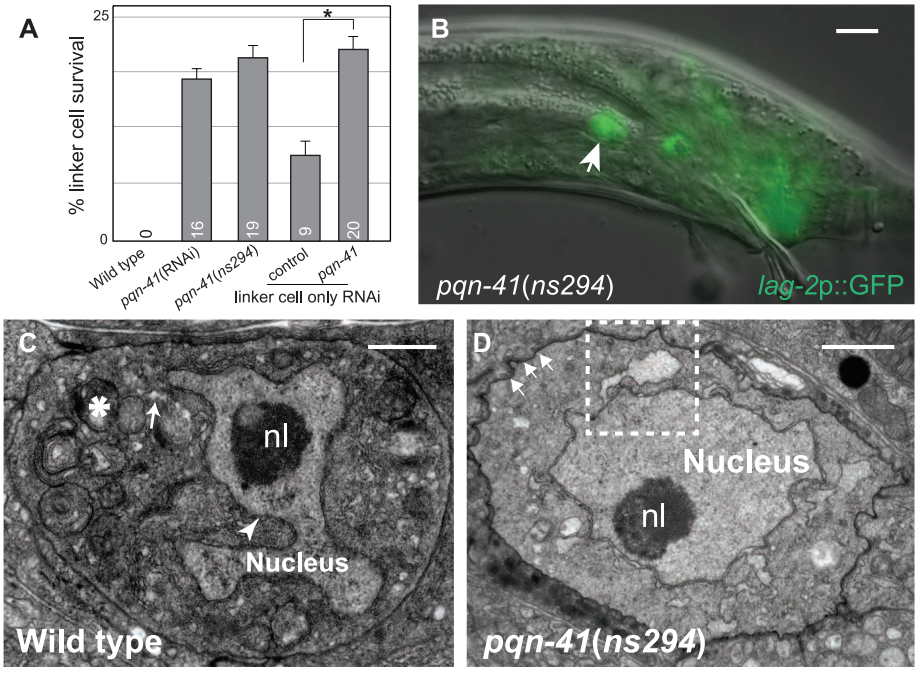


**Fig. 1.** PQN-41 is required for linker cell death. (**A**) Linker cell survival 2 to 4 hours after the L4 molt. Numbers, percentages. Error bars indicate SEM. *$P$ < 0.04; $n \geq 50$ animals. Increased survival in *rde-1* may reflect reduced *let-7* miRNA function (*8*). (**B**) Adult *pqn-41*(*ns294*) male with surviving linker cell (arrow). Scale bar, 10 μm. (**C**) Electron micrograph of dying linker cell in a wild-type animal. nl, nucleolus. Arrow indictaes swollen ER, asterisk indicates mitochondria, and arrowhead indicates nuclear envelope crenellation. (**D**) Electron micrograph of linker cell in (B). Arrows indicate adhesion junctions. Dashed box is enlarged in fig. S2A. Scale bars in (C) and (D), 2 μm.

as observed with light microscopy. To examine surviving linker cell morphology at higher resolution, we performed serial-section EM. We found that the cell forms adherens junctions to surrounding epithelia (*8*) and that nuclear envelope crenellation is mild ($n$ = 2 animals) (Fig. 1D). In both animals, however, organelle swelling was evident (Fig. 1D and fig. S2, A and B), suggesting that *pqn-41* may be required for nuclear crenellation but not organelle swelling.

To determine whether *pqn-41* functions cell-autonomously, we examined *rde-1*(*ne219*) RNAi–deficient mutants (*16*), containing a *mig-24* promoter::*rde-1* cDNA transgene restoring RNAi only in the linker cell (*17*). Feeding *pqn-41* RNAi bacteria to these mutants resulted in linker cell death defects similar to systemic RNAi (Fig. 1A), suggesting that *pqn-41* functions cell-autonomously. To further examine this issue, we assessed whether expression of *pqn-41* within the linker cell can restore linker cell death to *pqn-41*(*ns294*) mutants. The *pqn-41* locus encodes at least three alternate transcripts, which we designated *pqn-41*A, -B, and -C (Fig. 2). *pqn-41*A/B span the locus, differing by alternative in-frame exon b. *pqn-41*C mRNA initiates immediately upstream of exon b (Fig. 2B). We found that expression of *pqn-41*C is sufficient to promote linker cell demise in *pqn-41*(*ns294*) mutants (Fig. 2D), strongly suggesting that *pqn-41* functions cell autonomously to promote linker cell death.

*pqn-41*C encodes a protein composed of runs of glutamine residues with one to eight residues per run (Fig. 2C and fig. S3A). Of the 427 *pqn-41*C codons, 151 encode glutamine. The average number of nonglutamine amino acids interrupting adjacent glutamine residues in PQN-41C is 1.8 and is the second smallest in the *C. elegans* proteome (fig. S4). Glutamine-rich domains are hallmarks of some neurodegenerative disease (ND) proteins and of Q/N-rich prions (*18*). Both domain classes can adopt coiled-coil structures (*18*). Similarly, PQN-41C is predicted to contain six coiled-coil motifs demarcated by flanking prolines (CC1-6) (fig. S5). Three sequences outside the coiled-coil motifs are conserved among nematodes (CD1-3) (fig. S3B), as is the overall proportion of glutamines (38, 37, and 37% in *C. remanei*, *C. brenneri*, and *C. briggsae*, respectively).

ND and Q/N-rich polyglutamine proteins tend to aggregate in cells (*18*). Similarly, we found that a PQN-41C::GFP protein forms cytoplasmic aggregates in the linker cell (Fig. 3G), suggesting that PQN-41C shares structural features with these proteins. To understand the importance of the coiled-coil and conserved regions to PQN-41C function, we examined the effects of protein truncations on the ability of PQN-41C to rescue *pqn-41*(*ns294*) mutants (fig. S6A). Truncation of consecutive pairs of coiled-coil domains abolishes PQN-41C rescuing activity. Coil-breaking prolines in coiled-coil domains 2, 4, and 6 also reduce rescue efficiency. Thus, sequences encoding the coiled-coil regions are

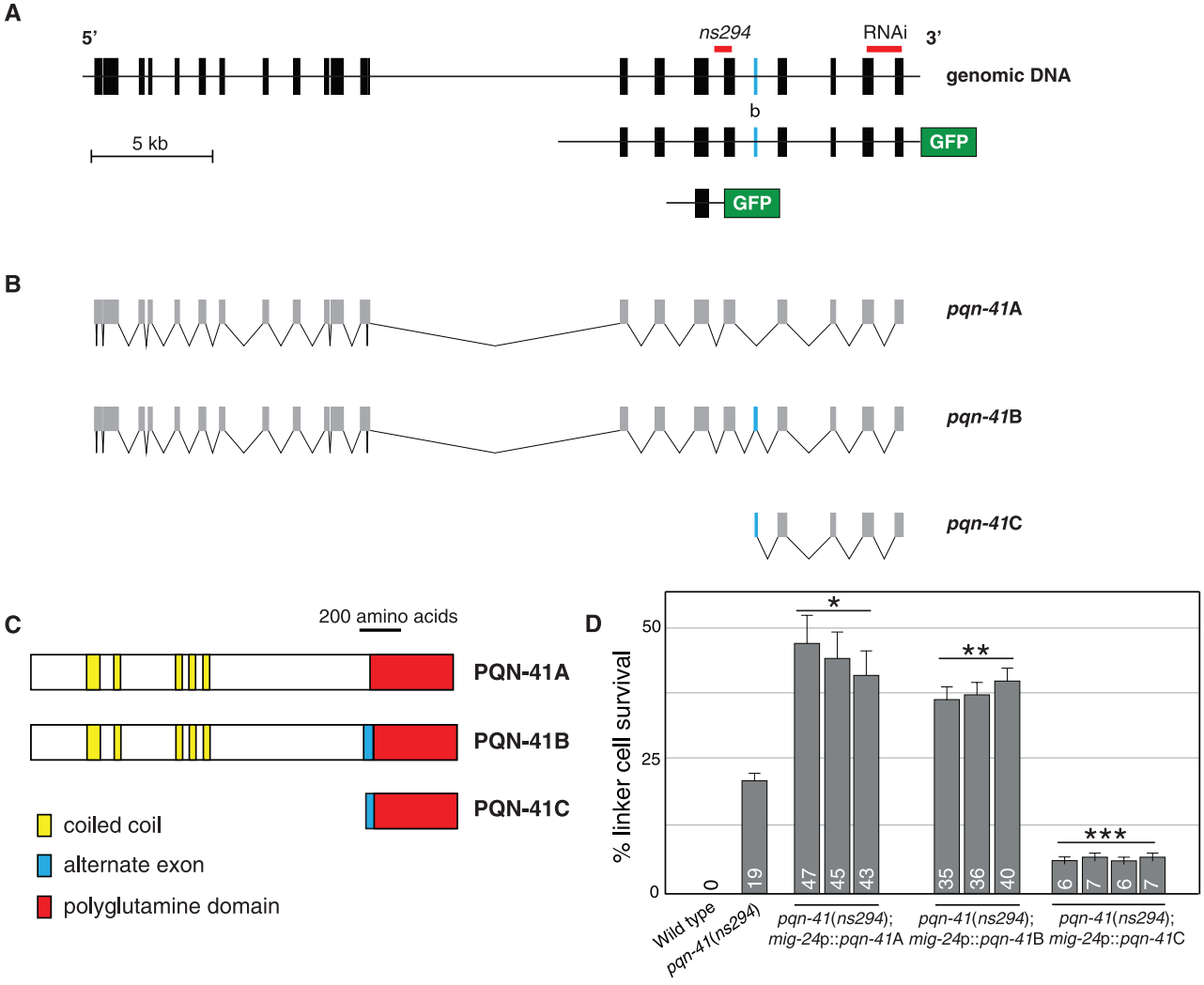


**Fig. 2.** PQN-41C promotes linker cell death. (**A**) *pqn-41* genomic region. Alternative exon b is labeled with the letter "b." GFP not to scale. (**B**) Three mRNAs generated by the *pqn-41* region. (**C**) Predicted protein structures for mRNAs in (B). (**D**) Linker cell survival in *pqn-41*(*ns294*) mutants expressing the indicated cDNAs. Numbers are percentages. Error bars indicate SEM. Asterisks signify different from *pqn-41*(*ns294*): *$P$ < 0.0009, $n$ = 138 animals; **$P$ < 0.0007, $n$ = 236 animals; ***$P$ < 0.004, $n$ = 229 animals.

important for PQN-41C function. Truncation of conserved domain CD3 also abolishes rescue, whereas deletion of the CD1/2 domains has only modest effects.

Expression of polyglutamine repeats is often toxic. However, PQN-41C does not exhibit nonspecific cellular toxicity. Expression of PQN-41C in the linker cell of *pqn-41*(*ns294*) males starting in L2 larvae did not cause precocious cell death ($n$ = 227 animals). Rather, cell death was initiated appropriately at the L4-adult transition. Likewise, expression of PQN-41C in the hermaphrodite distal tip cells or the anchor cell did not kill these cells ($n$ > 38 animals for each). Thus, PQN-41C requires the appropriate cellular context to promote death.

To investigate the functions of the *pqn-41*A/B transcripts, we tested whether they could restore linker cell death to *pqn-41*(*ns294*) mutants. We found that both transcripts enhance linker cell survival in *pqn-41*(*ns294*) (Fig. 2D) and wild-type animals (fig. S6B). Although other polyglutamine proteins can protect cells from polyglutamine toxicity (*19*), it is puzzling that PQN-41A/B protect the linker cell, given that both proteins contain the glutamine-rich sequences of PQN-41C. It is possible that the N terminus of PQN-41A/B overrides the cell death–promoting activity of the glutamine-rich domain. Supporting this idea, the N terminus is sufficient to block linker cell death (fig. S6B). Furthermore, PQN-41A/B::GFP proteins expressed in the linker cell fail to aggregate (Fig. 3, E and F).

ND and Q/N-rich proteins often contain coiled-coil motifs outside the glutamine-rich domain or associate with proteins containing such domains (*18*). Similarly, PQN-41A and -B N-termini are predicted to contain at least five coiled-coil motifs (fig. S7). We found, however, that deletion of sequences encoding different coiled-coil domains did not abolish ectopic survival induced by *pqn-41*B (fig. S6B).

We next sought to characterize *pqn-41* expression. A 13-kb DNA fragment derived from the *pqn-41* locus and fused to *gfp* sequences is broadly expressed in transgenic animals in most cells starting in the embryo (Figs. 2A and 3). However, expression is only switched on in the linker cell as the cell begins to die (Fig. 3, A to D). A 2.5-kb DNA subfragment derived from this reporter promotes *gfp* expression nearly exclusively in the linker cell, and only upon cell death initiation (Fig. 2A and fig. S8). The sequences driving linker cell expression of *pqn-41* overlap with those deleted in *pqn-41*(*ns294*) mutants and lie upstream of the *pqn-41*C start (Fig. 2A), suggesting that they may control *pqn-41*C expression.

We previously demonstrated a role for the LIN-29 zinc-finger transcription factor in linker cell death (fig. S9B) (*8*). *lin-29* is expressed in the linker cell before the cell begins to die, suggesting that *lin-29* might control *pqn-41* expression. However, *pqn-41* expression is only modestly disturbed in *lin-29*(RNAi) males (Fig. 4B and fig. S10A). To identify strong regulators of *pqn-41* expression, we tested clones identified in our RNAi screen. A clone directed against the gene *tir-1*—encoding a p38 mitogen-activated protein kinase (MAPK) scaffolding protein important for *C. elegans* innate immunity, neuronal differentiation, and stress responses (*20*, *21*)—blocks linker cell death, as does the *tir-1*(*qd4*) genetic lesion (fig. S9B). We tested whether other genes involved in innate immunity and stress affect linker cell death. Two independent alleles of the p38 cascade MAPKK gene *sek-1* strongly block linker cell death (Fig. 4A, fig. S9, and table S2); however, none of the other genes we tested had an effect (table S2). Thus, *sek-1* promotes linker cell death independently of innate immunity, stress response, and neuronal differentiation pathways. Unlike in *lin-29*(RNAi) animals, *pqn-41* expression is often not detected in *sek-1* mutants (Fig. 4B), suggesting that *sek-1* functions upstream of *pqn-41*. Consistent with this idea, double mutants carrying a strong loss-of-function lesion in *sek-1* and the *pqn-41*(*ns294*) allele have a survival defect similar to that of *sek-1* mutants alone (fig. S9B). Furthermore, EM of surviving linker cells in *sek-1*(*ag1*) mutants reveals no nuclear crenellation, but some endoplasmic reticulum (ER) swelling ($n$ = 2 animals) (Fig. 4C), which is consistent with regulation of *pqn-41* by *sek-1*. The differential effects of *lin-29* and *sek-1* on *pqn-41* expression suggest that these genes function independently. Indeed, we found that *sek-1* expression does not require *lin-29* function, and vice versa (fig. S10, B and C). Furthermore, *lin-29* mutants do not exhibit the extent of ER swelling of *sek-1* mutants ($n$ = 3 animals) (fig. S11). Last, strong loss-of-function mutations in *lin-29* and *sek-1* interact additively (fig. S9B), suggesting that these genes may indeed function in parallel.

To determine where *sek-1* functions, we examined its expression using a *sek-1* genomic region::GFP reporter. This transgene was expressed in the linker cell throughout the cell's development (Fig. 4D). Expression of a *sek-1* cDNA using the *mig-24* linker cell–specific promoter restored cell death in *sek-1* mutants to a greater extent than did expression of *sek-1* using the *lin-48* promoter, which is active in surrounding cells (Fig. 4A) (*22*). These results support a cell-autonomous role for *sek-1* in linker cell death.

The studies described here—as well as the morphological similarities between linker cell death and vertebrate developmental cell death—raise the possibility that PQN-41–like proteins might mediate nonapoptotic developmental cell death in vertebrates. The vertebrate proteins MED12

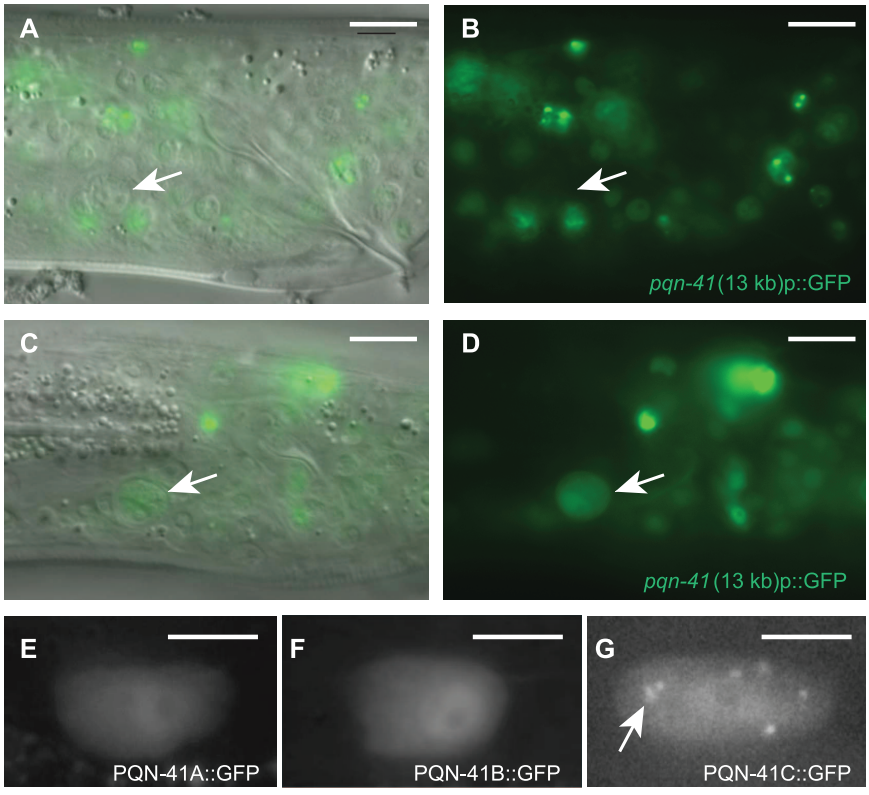


**Fig. 3.** PQN-41 is expressed as the linker cell dies. (**A**) Differential interference contrast and fluorescence image of late L4 male expressing the 13 kb *pqn-41*::GFP reporter in Fig. 2A. Arrow indicates linker cell. (**B**) Fluorescence image only. (**C**) Same as (A) except in an older L4 animal. (**D**) Fluorescence image only. (**E** to **G**) Expression of *mig-24* promoter::*pqn-41*A, -B, and -C cDNA GFP translational fusions, respectively. Arrow indicates cytoplasmic puncta. Scale bars, 10 μm [(A) to (D)], 5 μm [(E) to (G)].

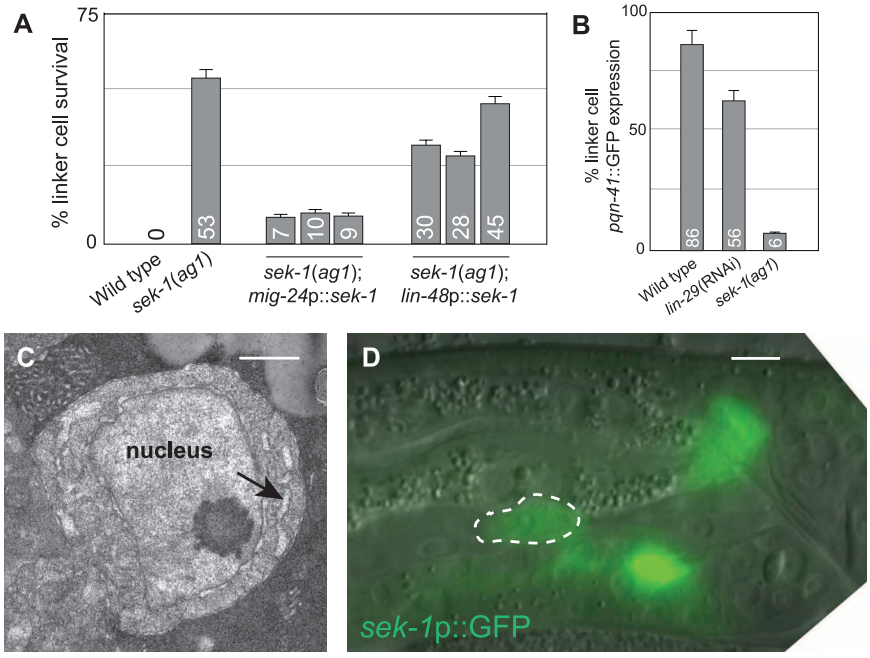


**Fig. 4.** SEK-1 MAPKK is required for linker cell death. (**A**) Linker cell survival in *sek-1*(*ag1*) mutants expressing the indicated promoter::cDNA constructs. Numbers are percentages. Error bars indicate SEM; $n \geq 70$ animals. (**B**) Expression of the 2.5 kb *pqn-41*::GFP reporter in late L4 (wild-type) or young adult (*lin-29*, *sek-1*) animals ($n \geq 50$ animals). (**C**) Electron micrograph of linker cell in fig. S9A. Arrow indicates swollen ER. Scale bar, 2 μm. (**D**) Late L4 male expressing a *sek-1* promoter::GFP reporter. Dashed line, linker cell. Scale bar, 5 μm.

and p400 may be good candidates for such proteins. They are the most similar in primary sequence structure to PQN-41, contain glutamine-rich C termini (fig. S12), are nuclearly localized, and are important in tumor formation (*23*, *24*). Intriguingly, EM studies reveal that nuclear envelope crenellation is strongly associated with several polyQ expansion diseases (fig. S13). Our studies thus raise the possibility that these disease proteins might promote neurodegeneration by inappropriately activating a linker cell death–type process.

### References and Notes


1. M. C. Abraham, S. Shaham, *Trends Cell Biol.* **14**, 184 (2004).
2. Y. Fuchs, H. Steller, *Cell* **147**, 742 (2011).
3. J. F. Kerr, A. H. Wyllie, A. R. Currie, *Br. J. Cancer* **26**, 239 (1972).
4. N. Honarpour *et al.*, *Dev. Biol.* **218**, 248 (2000).
5. E. Coucouvanis, G. R. Martin, *Cell* **83**, 279 (1995).
6. W. Declercq, T. Vanden Berghe, P. Vandenabeele, *Cell* **138**, 229 (2009).
7. K. Newton, X. Sun, V. M. Dixit, *Mol. Cell. Biol.* **24**, 1464 (2004).
8. M. C. Abraham, Y. Lu, S. Shaham, *Dev. Cell* **12**, 73 (2007).
9. J. E. Sulston, D. G. Albertson, J. N. Thomson, *Dev. Biol.* **78**, 542 (1980).
10. H. M. Ellis, H. R. Horvitz, *Cell* **44**, 817 (1986).
11. G. Pilar, L. Landmesser, *J. Cell Biol.* **68**, 339 (1976).
12. R. W. Oppenheim *et al.*, *J. Neurosci.* **21**, 4752 (2001).
13. T. Borsello, V. Mottier, V. Castagné, P. G. Clarke, *J. Comp. Neurol.* **453**, 361 (2002).
14. F. Simmer *et al.*, *Curr. Biol.* **12**, 1317 (2002).
15. R. E. Ellis, H. R. Horvitz, *Development* **112**, 591 (1991).
16. H. Tabara *et al.*, *Cell* **99**, 123 (1999).
17. K. K. Tamai, K. Nishiwaki, *Dev. Biol.* **308**, 562 (2007).
18. F. Fiumara, L. Fioriti, E. R. Kandel, W. A. Hendrickson, *Cell* **143**, 1121 (2010).
19. P. W. Faber, C. Voisine, D. C. King, E. A. Bates, A. C. Hart, *Proc. Natl. Acad. Sci. U.S.A.* **99**, 17131 (2002).
20. N. T. Liberati *et al.*, *Proc. Natl. Acad. Sci. U.S.A.* **101**, 6593 (2004).
21. C. F. Chuang, C. I. Bargmann, *Genes Dev.* **19**, 270 (2005).
22. A. D. Johnson, D. Fitzsimmons, J. Hagman, H. M. Chamberlin, *Development* **128**, 2857 (2001).
23. M. Fuchs *et al.*, *Cell* **106**, 297 (2001).
24. N. Mäkinen *et al.*, *Science* **334**, 252 (2011).


**Acknowledgments:** We thank J. Darnell and Shaham lab members for discussions; N. Tishbi for technical assistance; and D. Kim, C. Bargmann, M. Kinet, M. Kato, P. Sternberg, K. Nishiwaki, and K. Matsumoto for reagents. Some nematode strains used in this work were provided by the *Caenorhabditis* Genetics Center, funded by the National Center for Research Resources. E.S.B. is supported in part by the Rockefeller Women & Science Fellowship Program and NIH training grant CA09673. S.S. is supported by NIH grant R01HD042680.

### Supporting Online Material

www.sciencemag.org/cgi/content/full/335/6071/970/DC1
Materials and Methods
Figs. S1 to S13
Tables S1 and S2
References (*25*–*65*)

11 October 2011; accepted 4 January 2012
10.1126/science.1215156

# The Robustness and Restoration of a Network of Ecological Networks

**Michael J. O. Pocock,*† Darren M. Evans,‡ Jane Memmott**

Understanding species' interactions and the robustness of interaction networks to species loss is essential to understand the effects of species' declines and extinctions. In most studies, different types of networks (such as food webs, parasitoid webs, seed dispersal networks, and pollination networks) have been studied separately. We sampled such multiple networks simultaneously in an agroecosystem. We show that the networks varied in their robustness; networks including pollinators appeared to be particularly fragile. We show that, overall, networks did not strongly covary in their robustness, which suggests that ecological restoration (for example, through agri-environment schemes) benefitting one functional group will not inevitably benefit others. Some individual plant species were disproportionately well linked to many other species. This type of information can be used in restoration management, because it identifies the plant taxa that can potentially lead to disproportionate gains in biodiversity.

All species are embedded in complex networks of interactions (*1*). Modeling food webs, and more generally, species' interaction networks, has advanced the understanding of the robustness of ecosystems in the face of species loss (*1*, *2*). A key question, of applied relevance, is how the robustness of different species' interaction networks varies and whether it covaries. This is particularly important given the current rate of species' declines and extinctions (*3*) and its consequent impact on ecosystem function. Currently, understanding of species' interaction networks is mostly limited to partial subsets of whole ecosystems [but see (*4*, *5*)]. However, studying the interdependence of different networks is important (*6*) and can alter our perspective on network fragility, a fact already shown with nonecological examples (*7*). Moreover, this approach can be used to identify keystone species in the overall network; if these species are made

School of Biological Sciences, University of Bristol, Woodland Road, Bristol BS8 1UG, UK.

*To whom correspondence should be addressed. E-mail: michael.pocock@ceh.ac.uk
†Present address: NERC Centre for Ecology & Hydrology, Crowmarsh Gifford, Wallingford, Oxfordshire OX10 8BB, UK.
‡Present address: Department of Biological Sciences, Hardy Building, University of Hull, Cottingham Road, Hull HU6 7RX, UK.